

# Hybrid coupling optomechanically assisted nonreciprocal photon blockade

Yong-Pan Gao\*

*School of Electronic Engineering and the State Key Laboratory of Information Photonics and Optical Communications, Beijing University of Posts and Telecommunications, Beijing 100876, China*

Chuan Wang†

*School of Artificial Intelligence, Beijing Normal University, Beijing 100875, China*

(Dated: December 1, 2020)

The properties of open quantum system in quantum information science is now extensively investigated more generally by the research community as a fundamental issue for a variety of applications. Usually, the states of the open quantum system might be disturbed by the decoherence which will reduce the fidelity in the quantum information processing. So it is better to eliminate the influence of the environment. However, as part of the composite system, rational use of the environment system could be beneficial to quantum information processing. Here we theoretically studied the environment induced quantum nonlinearity and energy spectrum tuning method in the optomechanical system. And we found that the dissipation coupling of the hybrid dissipation and dispersion optomechanical system can induce the coupling between the environment and system in the cross-Kerr interaction form. When the symmetry is broken with a directional pumping environment, the system exhibits the non-reciprocal behavior during the photon excitation and photon blockade for the clockwise and counterclockwise modes of the whispering-gallery mode microcavity. Furthermore, we believe that the cross-Kerr coupling can also be used in a more widely region in quantum information processing and quantum simulation.

## I. INTRODUCTION

Quantum information processing and quantum metrology rely on the efficient manipulation of the qubits which have attracted intense interest during the past decades. It has been found that the system for quantum information processing are not isolated and may be characterized by the open quantum system. Furthermore, the decoherence of the environment may induce noise and reduce the fidelity of the quantum states. On the other hand, the rational use of the environment system may be beneficial to the quantum system. Here we are intending to investigate the dynamics of the dissipation process based on the cavity optomechanical system. Recently, cavity optomechanical system is introduced into the study of quantum information science. Cavity optomechanical system [1–6] is an artificial microstructure that combines the interaction between the mechanical mode and the optical mode with various effect could be observed on it. For example, the optomechanical induced transparency [7–16], optomechanical assisted nonlinearity [17–26], phonon lasers [27–32], in the semi-classical region; the photon blockade [33–39], mechanical resonator cooling [40–45], nonclassical state preparation [46–54], and the fundamental quantum properties [55–59] in the full quantum region.

The geometric deformation characteristics of the optomechanics and the geometric deformation correlation of its optical properties endow the optical machine with unique and excellent physical properties. Different from other systems, such as the cavity-atom coupled system

[60–64] and cavity-magnetic coupled system [65–69], optomechanics provides us a platform to investigate the properties of the non-static coupling between the system and the environment. The dissipative optomechanics describes the coupling of the optical mode to the environment of a cavity [70–77], when it is combined with the dispersion optomechanics [7, 9–11], the hybridization of the dissipative optomechanics with the dispersion optomechanics shows potential applications in pure optical manipulation. The hybrid systems have become a key strategy in microwave electromechanical system [78–82]. Recently, various studies have shown that such kind of optomechanical system with both dispersive coupling and dissipative coupling can be realized in the whispering-gallery cavities [83–88].

In this study, we present a full quantum approach that describes the dissipation and dispersion hybrid coupled optomechanical system. First, we developed the self-Kerr effect based on the dispersive coupling, and illustrated the cross-Kerr effect of the environment caused by dissipative coupling on the system. In order to show the potential applications of the cross Kerr effect, relying on the directional coherent manipulation of the cross-Kerr interaction, this approach is further applied to achieve the tunable non-reciprocity between the intrinsic optical clockwise and counter-clockwise modes, and also the non-reciprocal photon blockade.

## II. THE DISSIPATION-DISPERSION HYBRID OPTOMECHANICS

The system is shown in FIG.1, the whispering-gallery mode (WGM) microcavity supports both the optical

\* gaoyongpan@bupt.edu.cn

† wangchuan@bnu.edu.cn

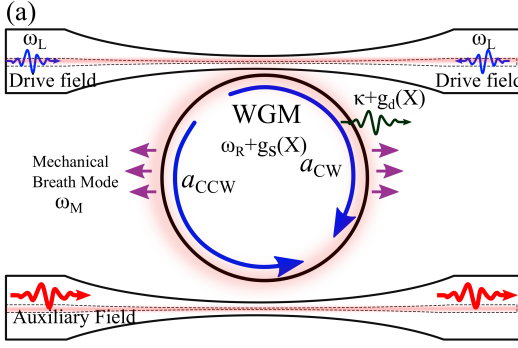


FIG. 1. The hybrid coupling optomechanics and its energy level scheme. The whisper gallery mode (WGM) has an unstable frequency  $\omega_R + g_s(X)$  and dissipation  $\kappa + g_d(X)$ . Both the clockwise (CW) and counterclockwise (CCW) of this WGM can be excited. An auxiliary field is weakly coupled with the CCW mode and tuning its resonant features through the dissipation induced cross-kerr effect. Here we studied the quantum feature of the weak drive field which is strong coupled with the cavity with the frequency  $\omega_L$ .

mode and the mechanical breath mode. Due to the optomechanical interaction, the mechanical breath mode will change both the curvature [89] and effective length of the microcavity, in which the dissipation and dispersion hybrid coupling optomechanics appears. The mechanical mode has the resonant frequency of  $\omega_M$  and negligible damping rate, while the optical mode has the position dependent frequency  $\omega_R + g_s(X)$  and dissipation rate  $\kappa + g_d(X)$ . The optomechanical microcavity is coupled with the add-drop fiber tapers. For the two fiber waveguides, the add fiber is strongly coupled with the cavity, and the weak driving field is input and output with the frequency  $\omega_L$  through this fiber; the drop fiber is weakly coupled with the cavity (The feed back of the cavity is negligible), the input field plays the role of controllable environment which is defined as the auxiliary field. The Hamiltonian of the dissipation-dispersion hybrid optomechanical system in FIG.1 could be expressed as (with  $\hbar = 1$ )

$$\hat{H} = \omega_R \hat{a}^\dagger \hat{a} + \omega_M \hat{c}^\dagger \hat{c} + \sum_q \omega_q \hat{b}_q^\dagger \hat{b}_q + \hat{H}_d + \hat{H}_s + \hat{H}_\gamma \quad (1)$$

Here the optical mode has the frequency of  $\omega_R$  with the annihilation operator denoted as  $\hat{a}$ .  $\hat{c}$  denotes the annihilation operator of the mechanical mode whose frequency is  $\omega_M$ .  $\hat{b}_q$  is the annihilation operator of the environment with the frequency  $\omega_q$ . And  $H_d$  corresponds to the dissipation coupling Hamiltonian,  $H_s$  represents the dispersion coupling Hamiltonian, and  $H_\gamma$  shows the dissipation part of the system. The present system could be achieved both in the microwave electro-mechanical system [78] and optical WGM system. The microwave system offer easy manipulation and processing, yet have limited thermal noise, while the present system enlarge the hybrid optomechanics from the microwave to optical wavelength. It can have much less thermal noise than the microwave

case, but is usually hard to approach the strong coupling regime of the system because the co-existence of the dissipation and the dispersion coupling.

The dissipative optomechanical coupling part could be described as

$$\hat{H}_d = g_d(X) \equiv X \frac{d\kappa}{dx} (\hat{b}_q \hat{a}^\dagger - \hat{b}_q^\dagger \hat{a}). \quad (2)$$

here  $X = \hat{c}^\dagger + \hat{c}$ , and the dispersion coupling term is

$$\hat{H}_s = g_s(X) \hat{a}^\dagger \hat{a} = g_s \hat{X} \hat{a}^\dagger \hat{a}. \quad (3)$$

For simplicity, we set  $\hat{A}^\dagger = \sum_q \hat{b}_q \hat{a}^\dagger$ . And the Hamiltonian could be written as

$$\hat{H} = \frac{\omega_R}{\hat{n}_q} \hat{a}^\dagger \hat{a} + \omega_M \hat{c}^\dagger \hat{c} + X [i g_d (\hat{A}^\dagger - \hat{A}) + \frac{g_s}{\hat{n}_q} \hat{A}^\dagger \hat{A}]. \quad (4)$$

As  $\hat{n}_q = \sum_q \hat{b}_q^\dagger \hat{b}_q$ , we assignment the above Hamiltonian as

$$\hat{H}_0 = \Omega_R \hat{A}^\dagger \hat{A} + \omega_M \hat{c}^\dagger \hat{c}, \quad (5a)$$

$$\hat{W} = X \left[ i g_d (\hat{A}^\dagger - \hat{A}) + \frac{g_s}{\hat{n}_q} \hat{A}^\dagger \hat{A} \right], \quad (5b)$$

$$\hat{H} = \hat{H}_0 + \hat{W}. \quad (5c)$$

By choosing the quadrature amplitudes as  $\hat{P} = i(\hat{A}^\dagger - \hat{A})$  and  $\hat{Q} = \hat{A}^\dagger + \hat{A}$ , then we have

$$\hat{W} = X [g_d \hat{P} + \frac{g_s}{4|B|^2} (\hat{Q}^2 + \hat{P}^2)]. \quad (6)$$

With the definition as  $B = \langle \sum_q \hat{b}_q \rangle$ , we perform the transformation by using the operator  $U_1 = e^{S_1}$ , where  $S_1 = i \frac{g_d |B|^2}{g_s} (\hat{A}^\dagger + \hat{A})$ . Then we can get

$$\begin{aligned} \hat{H} &= \frac{\Omega_R}{\hat{n}_p} (A - i \frac{g_d \hat{n}_q}{g_s}) (A^\dagger + i \frac{g_d \hat{n}_q}{g_s}) + \omega_M \hat{c}^\dagger \hat{c} \\ &+ X \left[ \frac{g_s}{\hat{n}} \hat{A}^\dagger \hat{A} + \frac{g_d^2 \hat{n}_q}{g_s} \right], \end{aligned} \quad (7)$$

here the term  $\hat{A} - \hat{A}^\dagger$  is the environment driven term that can be eliminated by the out-phase drive. Then, the Hamiltonian of the system could be changed to

$$\hat{H} = \frac{\Omega_R}{\hat{n}} \hat{A}^\dagger \hat{A} + \omega_M \hat{c}^\dagger \hat{c} + X \left[ \frac{g_s}{\hat{n}} \hat{A}^\dagger \hat{A} + \frac{g_d^2 \hat{n}_q}{g_s} \right]. \quad (8)$$

The environment is single mode  $\hat{n}_q = \hat{b}^\dagger \hat{b}$ . Then by using the transformation operator  $S_2 = \exp(\hat{c}^\dagger - \hat{c}) (\frac{g_s}{\hat{n}} \hat{A}^\dagger \hat{A} + \frac{g_d^2 \hat{n}_q}{g_s})$ , the system could be changed to

$$\hat{H} = \left( \omega_R - \frac{g_s^2}{\omega_M} \hat{a}^\dagger \hat{a} - \frac{2g_d^2}{\omega_M} \hat{b}^\dagger \hat{b} \right) \hat{a}^\dagger \hat{a} + \omega_M \hat{c}^\dagger \hat{c}. \quad (9)$$

Previously, the cross-Kerr effect is usually discussed in the semi-classical region which induced directly [90–93]. For example, the cross-Kerr effect between the mechanical mode and optical mode [94, 95]. Here we consider the cross-Kerr nonlinearity as a port which is open to the environment, and provides us a tool for the control of the cavity.

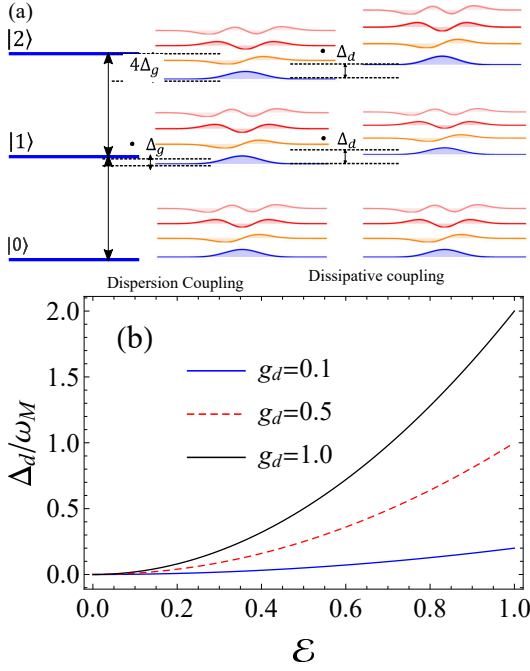


FIG. 2. The energy scheme and shift of the hybrid optomechanical system. (a). How the dispersion and dissipation coupling modulation the energy scheme. (b). The energy shift  $\Delta_d$  varies with the auxiliary field strength  $\mathcal{E}$  under different dissipation coupling strength  $g_d/\omega_M = 0.1, 0.5, 1$ .

### III. ENERGY STRUCTURE AND ITS MODULATION WITH THE AUXILIARY FIELD

As the environment plays the role of the cross-Kerr term, in order to study the dynamics of the system, here an auxiliary field is introduced to simulate the environment which is stronger than the driving field. The environment for the directional features of the CW and CCW fields are different for the field in the waveguide.

The pump strength of the auxiliary field on the cavity is set as  $\mathcal{E}$ , then frequency shift of the CCW mode could be denoted as  $\frac{2g_d^2\mathcal{E}^2}{\omega_M}\langle\alpha|\hat{b}^\dagger\hat{b}|\alpha\rangle$  according to Eq.9.  $|\alpha\rangle$  represents the coherent state. Here it is obvious that the frequency shift is different in the CW and CCW directions. We assume the intensity of the probe beam is weaker compared with the pumping beam. And the probe beam is bidirectional, the pumping beam is only coupled with the CW mode. Then the Hamiltonian of the two modes could be expressed as

$$\hat{H}_{CW} = \left( \omega_R - \frac{g_s^2}{\omega_M} \hat{a}_{CW}^\dagger \hat{a}_{CW} - \frac{2g_d^2}{\omega_M} \mathcal{E}^2 \right) \hat{a}_{CW}^\dagger \hat{a}_{CW} + \omega_M \hat{c}^\dagger \hat{c}, \quad (10a)$$

$$\hat{H}_{CCW} = \left( \omega_R - \frac{g_s^2}{\omega_M} \hat{a}_{CCW}^\dagger \hat{a}_{CCW} \right) \hat{a}_{CCW}^\dagger \hat{a}_{CCW} + \omega_M \hat{c}^\dagger \hat{c}. \quad (10b)$$

From Eq.10, we can find frequency shift of both the CW

and CCW modes are related to the intensity of the auxiliary field. And the eigen-energy of the two modes could be solved as

$$E_{n,CW} = n\hbar\omega_R - \frac{g_s^2}{\omega_M} n^2 - \frac{2g_d^2}{\omega_M} \mathcal{E}^2 + n_M \omega_M, \quad (11a)$$

$$E_{n,CCW} = n\hbar\omega_R - \frac{g_s^2}{\omega_M} n^2 + n_M \omega_M. \quad (11b)$$

As shown in FIG.2, the energy-level structure generation of our scheme is presented. Except that the energy level distribution is no longer uniform, the mechanical system will generate many mechanical sub-level which is different from the pure Kerr case. Thus, the dispersion coupling will shift the energy level with different amplitude and there are several mechanical dressed energy level generated. Then the energy could be shifted by the dissipation coupling generation, and the variance is related to the auxiliary field strength. In FIG.2 (b) we show the frequency shift varies with the auxiliary field strength  $\mathcal{E}$  under the dissipation coupling strength of  $g_d = 0.1, 0.5, 1$ .

### IV. THE PHOTON EXCITATION AND PHOTON BLOCKADE OF THE HYBRID COUPLING SYSTEM

As the energy gap is no longer equally spaced and auxiliary field is adjustable, the non-reciprocal photon blockade could be achieved in our hybrid coupling system. The dynamical equation of the system without environment noise is

$$\dot{\hat{a}}(t) = (i\Delta_i - \kappa)\hat{a}_i(t) + e^{-iP(t)}\mathcal{E}_p + \mathcal{O}(\mathcal{E}_p^2 a_{in}). \quad (12)$$

Here,  $i$  denotes the mode CW or CCW. The detunings are  $\Delta_{CW} = \Delta - \frac{g_{der}^2}{\omega_M} - \frac{2g_{dis}^2}{\omega_M} \mathcal{E}^2$ ,  $\Delta_{CCW} = \Delta - \frac{g_{der}^2}{\omega_M}$ , and  $\Delta = \omega_L - \omega_R$  is the detuning of the laser from the bare cavity frequency.  $P(t) = e^{-iH_m t} P e^{iH_m t}$ ,  $H_m = \omega_M \hat{c}^\dagger \hat{c}$  is the free mechanical Hamilton. Here we assume the pumping beam is the environment which is not affected by the feedback. By integrating Eq.12 under the weak driven condition, we find the spectrum function of the system could be solved as [33, 34, 96–98]:

$$S(\Delta) \simeq \kappa \sum_{n=-\infty}^{\infty} A_n \frac{\kappa_n}{\kappa_n^2 + (\Delta_i - n\omega_m)^2}, \quad (13)$$

where  $A_n = e^{-\eta^2(2N+1)} I_n [2\eta^2 \sqrt{N(N+1)}] ((N+1)/N)^{n/2}$ .  $N$  denotes the total photon number, in which  $N(\omega) = 1/(e^{\hbar\omega/k_B T} - 1)$  for the thermal state,  $k_B$  is the Boltzmann constant.

To further clarify the properties of the hybrid coupling system, we show the photon excitation spectrum in FIG.3. Here the black line represents the photon excitation of CW mode, while the red and blue line show the auxiliary field shift photon excitation spectrum of

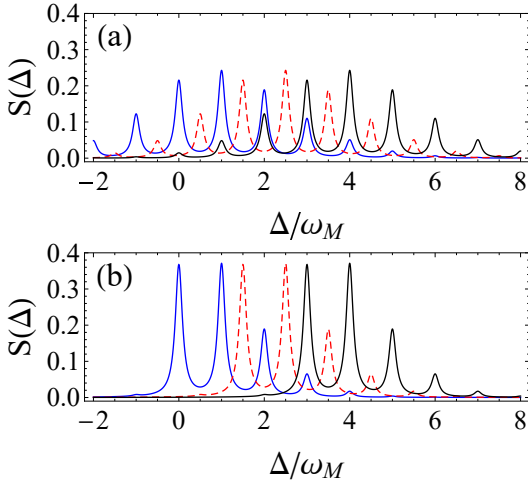


FIG. 3. The photon number shift with high thermal phonon number and lower photon number. (a). The photon excitation spectrum varies with frequency detuning  $\Delta$  under 1 thermal phonon environment. (b). The photon excitation spectrum varies with frequency detuning  $\Delta$  under 0.01 thermal phonon environment. In both figures, we have  $\kappa/\omega_M = 0.1$ , the quality factor of the mechanical mode is  $10^4$ , and the dispersion coupling strength  $g_s/\omega_M = 1$ . The shift strength is  $\Delta_d/\omega_M = 0.5$  for the red line, while it is 1 for the black line.

the CCW mode. In figure FIG.3(a), the thermal photon number is set as 1. We can find that there are resonance peaks at both the positive and negative detuning regions. When the thermal photon number is chosen as 0.01 in FIG.3 (b), there are only resonance peaks in the positive detuning region. It is because the thermal noise will bridge different mechanical sub-levels.

One more important thing is that the auxiliary field will cause energy level displacement. Here we show the cross-Kerr induced shift  $\Delta_d = 0$ ,  $\Delta_d = 0.5\omega_m$  and  $\Delta_d = \omega_m$  with different lines in this figure, respectively. There are obviously spectrum shifts for both cases. However, the reciprocity of the excitation spectrum is different in FIG.3(a) and (b). When the thermal photon number is higher (1 thermal photon in the environment), the blue line and the black line are partially reciprocal when  $\Delta/\eta = 1$ , or 2, while it is fully reciprocal under the lower thermal environment condition. Moreover, we can also achieve full reciprocity by tuning the cross-Kerr induced frequency shift. When comparing the blue and red lines, we can find their peak points are alternately distributed. Then we can also achieve full reciprocity by choosing suitable  $\Delta$ .

Beyond the energy levels of the system, we also studied the properties of the correlation functions. The dynamical equation of the second-order term is

$$\dot{\hat{a}}^2(t) = 2(i\Delta_i + i\Delta_g - \kappa)\hat{a}^2(t) + \mathcal{E}_p e^{-iP(t)} a(t). \quad (14)$$

By integrating the above equation,  $a^2$  could be solved. Then, the second-order correction function  $g_i^{(2)}(0) =$

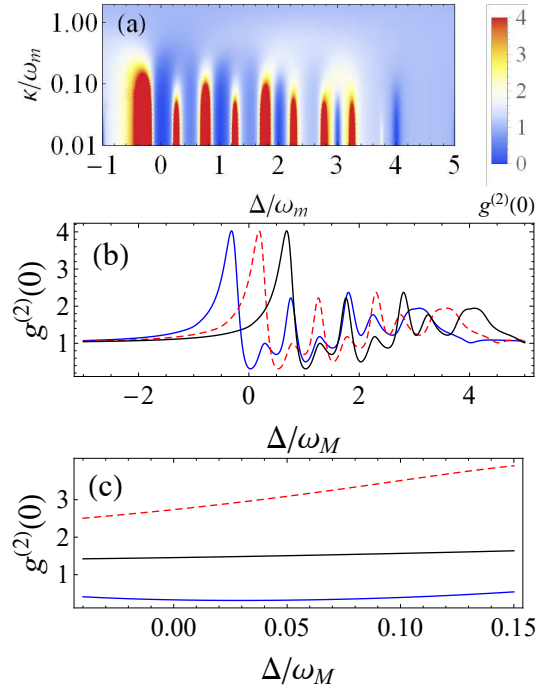


FIG. 4. The second correlation function and its shift of the hybrid optomechanics. (a). The second correlation function with 0.001 thermal phonons. (b). The correlation spectrum shift with the auxiliary field. The  $\kappa/\omega_M = 0.15$  and thermal phonon number is 0.001. We ignore the loss of mechanical mode. The shift strength is  $\Delta_d/\omega_M = 0.5$  for the red line, while it is 1 for the black line. (c). The zoom of (b).

$\langle a^{\dagger 2} a^2 \rangle / \langle a^\dagger a \rangle^2$  can be written as

$$g_i^{(2)}(0) = \text{Re} \sum_{n,m,p} \frac{B_{n,m,p}}{[\kappa + i(\Delta_i - n\omega_M)][\kappa - i(\Delta_i - m\omega_M)]} \times \frac{2\kappa^3}{[2\kappa - i(2\Delta_i + 2\Delta_g - p\omega_m)] S^2(\Delta)}. \quad (15)$$

For simplicity, we set the temperature is near zero, then we have  $B_{n,m,p} = e^{-2\eta^2} (\eta^2)^p W_{n,p}(\eta) W_{m,p}(\eta) / n! m! p!$ ,  $W_{n,p}(\eta) = (-1)^n U[-n, 1 - n + p, \eta^2]$ . The  $U[a, b, x]$  is a confluent hypergeometric function, and  $\eta = g_{der}/\omega_M$  is a dimensionless parameter.

According to the second-order correlation function given in Eq.15, the photon blockade characteristic of the hybrid optomechanical system is also studied. In FIG.4 (a), we report the theoretical calculations of the CW (black line) and CCW (red and blue line) correlation spectrum under different driving strength and cavity dissipation. We find that the second-order correlation function is almost zero when the detuning  $\Delta/\omega_M$  is 0, 1, 2, 3, 4 which displays the photon blockade, and it decreases along with the decrement of the parameter  $\kappa$ . So, we choose  $\kappa = 0.15$  as a key parameter in our study. Then the coherent environment can shift the  $g_i^{(2)}(0)$  of the CCW mode in FIG.4 (b). Thus, the non-

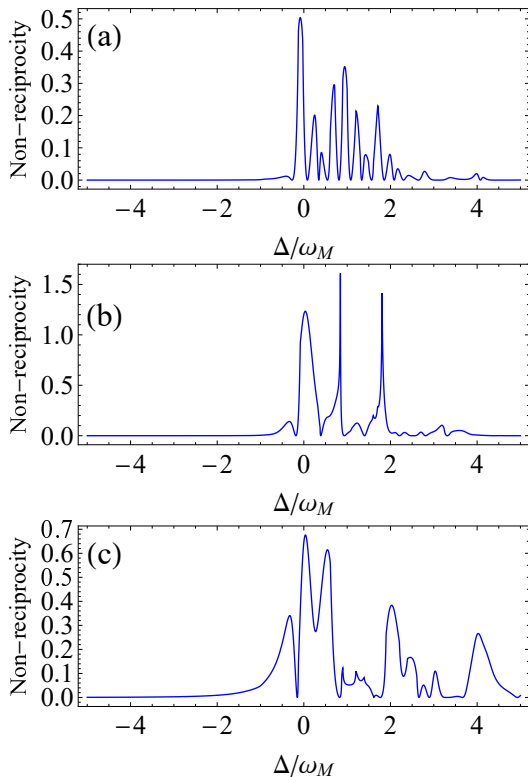


FIG. 5. The Non-Reciprocity under different environment pumping. (a). The shift is  $\Delta_d = 0.1$ . (b). The shift is  $\Delta_d = 0.5$ . (c). The shift is  $\Delta_d = 1$ . In all figures, we have  $\kappa/\omega_M = 0.15$ , the dispersion coupling strength  $g_s/\omega_M = 0.5$ , the thermal phonon numbers is 0.001, and the mechanical dissipation is neglected.

reciprocity could be achieved by choosing the parameter for the  $g^{(2)}(0)$ , we can easily achieve non-reciprocity. In order to show the non-reciprocity more obviously, we show its zoom in FIG.4 (c). However, the degree of non-reciprocity under different pumping strength is different. When the shift is  $0.5\omega_M$ , the  $g^{(2)}(0)$  is ranging between 1 and 2. When the shift is  $\omega_M$ , the  $g^{(2)}(0)$  is above 2. So, when we give a frequency as  $\omega_M$ , the system shows better performance of the non-reciprocity.

The non-reciprocal photon blockade is a part of the non-reciprocity feature of the second-order correlation function. To quantitatively study the nonreciprocal feature of the this system, we define the photon nonreciprocity as

$$\mathcal{R}(\Delta) = \frac{(\log(g_{CW}^{(2)}) - \log(g_{CCW}^{(2)}))^2}{|\log(g_{CW}^{(2)})| + |\log(g_{CCW}^{(2)})|}. \quad (16)$$

There, the denominator represents the sum of the correlation function of the CW and CCW mode, while the numerator is the size of their difference. We choose the logarithm operation of the correlation as the 1 is the decision point of photon correlation.

The performance of Eq.16 is shown in FIG.5. The coherent induced frequency shift is 0.1, 0.5, and 1 for the CCW mode, respectively. When the detuning is small as 0.1 as shown in FIG.5(a), the main peak appears in the near-zero region, while the maximal value is smaller than  $\log_{10}(4)$ . So the non-reciprocal photon blockade will not occur. While when we set the environment induced shift as 0.5, as shown in FIG.5(b), there are transmission peaks in the resonance position ( $\Delta/\omega_M = 0, 1, 2$ ). It is because the resonance dip in the transmission spectrum of the CCW mode is shifted to the peak of the CW mode, and the non-reciprocal photon blockade occur. When we continuously increasing the shift to 1, as shown in FIG.5(c), the maximal values of the non-reciprocity decreases, for the resonant peaks of the CW and CCW modes meet again. When we return to FIG.4(b)(c) again, we can find the non-reciprocity is not large as the Eq.16(b), but the non-reciprocal photon blockade can still occur.

## V. SUMMARY

In summary, we present a full quantum approach to study the dynamical behavior of the dissipation and dispersion coupled optomechanical system. The coupling would introduce the Kerr type nonlinearity, in particular, dissipative coupling will cause cross Kerr coupling between the cavity mode and the environment. On the other hand, by exploiting the cross-Kerr nonlinearity in the system, the non-reciprocity of the second-order correlation function on the CW and CCW propagation optical modes is illustrated. Moreover, we find the photon blockade effect on both the CW and the CCW propagation directions. Our research give an insight view of the environment of the whispering gallery mode in the full quantum region. When we simply apply this scheme to an coherent environment, is shows excellent photon non-reciprocal blocking performance which will be the powerful tool in the realization of quantum networking, nonlinear quantum gate, quantum information processing.

## VI. ACKNOWLEDGEMENTS

The authors gratefully acknowledge the support from the Fundamental Research Funds for the Central Universities(BNU) and the National Natural Science Foundation of China through Grants Nos. 61622103.

[1] W. P. Bowen and G. J. Milburn, *Quantum optomechanics* (CRC press, 2015).

[2] M. Aspelmeyer, T. J. Kippenberg, and F. Marquardt, *Cavity optomechanics: nano-and micromechanical res-*

- onators interacting with light* (Springer, 2014).
- [3] M. Aspelmeyer, T. J. Kippenberg, and F. Marquardt, Cavity optomechanics, *Rev. Mod. Phys.* **86**, 1391 (2014).
  - [4] T. Kippenberg and K. Vahala, Cavity opto-mechanics, *Opt. Express* **15**, 17172 (2007).
  - [5] T. J. Kippenberg and K. J. Vahala, Cavity optomechanics: back-action at the mesoscale, *science* **321**, 1172 (2008).
  - [6] G. Bahl, K. H. Kim, W. Lee, J. Liu, X. Fan, and T. Carmon, Brillouin cavity optomechanics with microfluidic devices, *Nature communications* **4**, 1 (2013).
  - [7] S. Weis, R. Rivière, S. Deléglise, E. Gavartin, O. Arcizet, A. Schliesser, and T. J. Kippenberg, Optomechanically induced transparency, *Science* **330**, 1520 (2010).
  - [8] A. Kronwald and F. Marquardt, Optomechanically induced transparency in the nonlinear quantum regime, *Phys. Rev. Lett.* **111**, 133601 (2013).
  - [9] H. Jing, Ş. K. Özdemir, Z. Geng, J. Zhang, X.-Y. Lü, B. Peng, L. Yang, and F. Nori, Optomechanically-induced transparency in parity-time-symmetric microresonators, *Scientific Reports* **5**, 9663 (2015).
  - [10] Y.-J. Zhu, C.-H. Bai, T. Wang, D.-Y. Wang, S. Zhang, and H.-F. Wang, Optomechanically induced transparency, amplification, and fast-slow light transitions in an optomechanical system with multiple mechanical driving phases, *Journal of the Optical Society of America B* **37**, 888 (2020).
  - [11] H. Lü, C. Wang, L. Yang, and H. Jing, Optomechanically induced transparency at exceptional points, *Phys. Rev. Applied* **10**, 014006 (2018).
  - [12] H. Lü, Y. Jiang, Y.-Z. Wang, and H. Jing, Optomechanically induced transparency in a spinning resonator, *Photonics Research* **5**, 367 (2017).
  - [13] M. Karuza, C. Biancofiore, M. Bawaj, C. Molinelli, M. Galassi, R. Natali, P. Tombesi, G. Di Giuseppe, and D. Vitali, Optomechanically induced transparency in a membrane-in-the-middle setup at room temperature, *Phys. Rev. A* **88**, 013804 (2013).
  - [14] C. Dong, J. Zhang, V. Fiore, and H. Wang, Optomechanically induced transparency and self-induced oscillations with bogoliubov mechanical modes, *Optica* **1**, 425 (2014).
  - [15] A. H. Safavi-Naeini, T. M. Alegre, J. Chan, M. Eichenfield, M. Winger, Q. Lin, J. T. Hill, D. E. Chang, and O. Painter, Electromagnetically induced transparency and slow light with optomechanics, *Nature* **472**, 69 (2011).
  - [16] G. S. Agarwal and S. Huang, Electromagnetically induced transparency in mechanical effects of light, *Phys. Rev. A* **81**, 041803 (2010).
  - [17] X. Wang, W. Qin, A. Miranowicz, S. Savasta, and F. Nori, Unconventional cavity optomechanics: Nonlinear control of phonons in the acoustic quantum vacuum, *Phys. Rev. A* **100**, 063827 (2019).
  - [18] T. F. Roque, F. Marquardt, and O. M. Yevtushenko, Nonlinear dynamics of weakly dissipative optomechanical systems, *New Journal of Physics* **22**, 013049 (2020).
  - [19] X.-Y. Lü, H. Jing, J.-Y. Ma, and Y. Wu,  $\mathcal{PT}$ -symmetry-breaking chaos in optomechanics, *Phys. Rev. Lett.* **114**, 253601 (2015).
  - [20] L. Bakemeier, A. Alvermann, and H. Fehske, Route to chaos in optomechanics, *Phys. Rev. Lett.* **114**, 013601 (2015).
  - [21] P. Djorwe, Y. Pennec, and B. Djafari-Rouhani, Frequency locking and controllable chaos through exceptional points in optomechanics, *Phys. Rev. E* **98**, 032201 (2018).
  - [22] H. Xiong, J. Gan, and Y. Wu, Kuznetsov-ma soliton dynamics based on the mechanical effect of light, *Phys. Rev. Lett.* **119**, 153901 (2017).
  - [23] M.-A. Miri, G. D'Aguanno, and A. Alù, Optomechanical frequency combs, *New Journal of Physics* **20**, 043013 (2018).
  - [24] C. Cao, S.-C. Mi, Y.-P. Gao, L.-Y. He, D. Yang, T.-J. Wang, R. Zhang, and C. Wang, Tunable high-order sideband spectra generation using a photonic molecule optomechanical system, *Scientific reports* **6**, 22920 (2016).
  - [25] Y.-P. Gao, T.-J. Wang, C. Cao, S.-C. Mi, D. Yang, Y. Zhang, and C. Wang, Effective mass sensing using optomechanically induced transparency in microresonator system, *IEEE Photonics Journal* **9**, 1 (2016).
  - [26] Y.-P. Gao, Z.-X. Wang, T.-J. Wang, and C. Wang, Optomechanically engineered phononic mode resonance, *Optics Express* **25**, 26638 (2017).
  - [27] C. Galland, N. Sangouard, N. Piro, N. Gisin, and T. J. Kippenberg, Heralded single-phonon preparation, storage, and readout in cavity optomechanics, *Phys. Rev. Lett.* **112**, 143602 (2014).
  - [28] B. Wang, Z.-X. Liu, X. Jia, H. Xiong, and Y. Wu, Polarization-based control of phonon laser action in a parity time-symmetric optomechanical system, *Communications Physics* **1**, 1 (2018).
  - [29] H. Lü, S. K. Özdemir, L.-M. Kuang, F. Nori, and H. Jing, Exceptional points in random-defect phonon lasers, *Phys. Rev. Applied* **8**, 044020 (2017).
  - [30] H. Jing, S. K. Özdemir, X.-Y. Lü, J. Zhang, L. Yang, and F. Nori,  $\mathcal{PT}$ -symmetric phonon laser, *Phys. Rev. Lett.* **113**, 053604 (2014).
  - [31] Y. Jiang, S. Maayani, T. Carmon, F. Nori, and H. Jing, Nonreciprocal phonon laser, *Phys. Rev. Applied* **10**, 064037 (2018).
  - [32] Y.-L. Zhang, C.-L. Zou, C.-S. Yang, H. Jing, C.-H. Dong, G.-C. Guo, and X.-B. Zou, Phase-controlled phonon laser, *New Journal of Physics* **20**, 093005 (2018).
  - [33] P. Rabl, Photon blockade effect in optomechanical systems, *Phys. Rev. Lett.* **107**, 063601 (2011).
  - [34] A. Nunnenkamp, K. Børkje, and S. M. Girvin, Single-photon optomechanics, *Phys. Rev. Lett.* **107**, 063602 (2011).
  - [35] J.-Q. Liao and F. Nori, Photon blockade in quadratically coupled optomechanical systems, *Phys. Rev. A* **88**, 023853 (2013).
  - [36] B. Li, R. Huang, X. Xu, A. Miranowicz, and H. Jing, Nonreciprocal unconventional photon blockade in a spinning optomechanical system, *Photonics Research* **7**, 630 (2019).
  - [37] D.-Y. Wang, C.-H. Bai, S. Liu, S. Zhang, and H.-F. Wang, Distinguishing photon blockade in a  $\mathcal{PT}$ -symmetric optomechanical system, *Phys. Rev. A* **99**, 043818 (2019).
  - [38] B. Sarma and A. K. Sarma, Unconventional photon blockade in three-mode optomechanics, *Phys. Rev. A* **98**, 013826 (2018).
  - [39] R. Huang, A. Miranowicz, J.-Q. Liao, F. Nori, and H. Jing, Nonreciprocal photon blockade,

- Phys. Rev. Lett. **121**, 153601 (2018).
- [40] Y.-C. Liu, Y.-F. Xiao, X. Luan, and C. W. Wong, Dynamic dissipative cooling of a mechanical resonator in strong coupling optomechanics, Phys. Rev. Lett. **110**, 153606 (2013).
- [41] M. Vanner, J. Hofer, G. Cole, and M. Aspelmeyer, Cooling-by-measurement and mechanical state tomography via pulsed optomechanics, Nature communications **4**, 1 (2013).
- [42] A. Nunnenkamp, K. Børkje, and S. M. Girvin, Cooling in the single-photon strong-coupling regime of cavity optomechanics, Phys. Rev. A **85**, 051803 (2012).
- [43] D.-G. Lai, F. Zou, B.-P. Hou, Y.-F. Xiao, and J.-Q. Liao, Simultaneous cooling of coupled mechanical resonators in cavity optomechanics, Phys. Rev. A **98**, 023860 (2018).
- [44] J.-Q. Liao and C. K. Law, Cooling of a mirror in cavity optomechanics with a chirped pulse, Phys. Rev. A **84**, 053838 (2011).
- [45] H.-K. Lau and A. A. Clerk, Ground-state cooling and high-fidelity quantum transduction via parametrically driven bad-cavity optomechanics, Phys. Rev. Lett. **124**, 103602 (2020).
- [46] J.-Q. Liao and L. Tian, Macroscopic quantum superposition in cavity optomechanics, Phys. Rev. Lett. **116**, 163602 (2016).
- [47] J.-Q. Liao, J.-F. Huang, and L. Tian, Generation of macroscopic schrödinger-cat states in qubit-oscillator systems, Phys. Rev. A **93**, 033853 (2016).
- [48] M. Wang, X.-Y. Lü, Y.-D. Wang, J. Q. You, and Y. Wu, Macroscopic quantum entanglement in modulated optomechanics, Phys. Rev. A **94**, 053807 (2016).
- [49] I. Shomroni, L. Qiu, and T. J. Kippenberg, Optomechanical generation of a mechanical catlike state by phonon subtraction, Phys. Rev. A **101**, 033812 (2020).
- [50] X.-Y. Lü, Y. Wu, J. R. Johansson, H. Jing, J. Zhang, and F. Nori, Squeezed optomechanics with phase-matched amplification and dissipation, Phys. Rev. Lett. **114**, 093602 (2015).
- [51] R. Ghobadi, S. Kumar, B. Pepper, D. Bouwmeester, A. I. Lvovsky, and C. Simon, Optomechanical micro-macro entanglement, Phys. Rev. Lett. **112**, 080503 (2014).
- [52] U. B. Hoff, J. Kollath-Bönig, J. S. Neergaard-Nielsen, and U. L. Andersen, Measurement-induced macroscopic superposition states in cavity optomechanics, Phys. Rev. Lett. **117**, 143601 (2016).
- [53] M. R. Vanner, M. Aspelmeyer, and M. S. Kim, Quantum state orthogonalization and a toolset for quantum optomechanical phonon control, Phys. Rev. Lett. **110**, 010504 (2013).
- [54] J. T. Muhonen, G. R. La Gala, R. Leijssen, and E. Verhagen, State preparation and tomography of a nanomechanical resonator with fast light pulses, Phys. Rev. Lett. **123**, 113601 (2019).
- [55] M. Zhou and S. M. Shahriar, Optomechanical resonator as a negative dispersion medium for enhancing the sensitivity bandwidth in a gravitational-wave detector, Phys. Rev. D **98**, 022003 (2018).
- [56] F. Armata, L. Latmiral, A. D. K. Plato, and M. S. Kim, Quantum limits to gravity estimation with optomechanics, Phys. Rev. A **96**, 043824 (2017).
- [57] V. Macri, A. Ridolfo, O. Di Stefano, A. F. Kockum, F. Nori, and S. Savasta, Nonperturbative dynamical casimir effect in optomechanical systems: Vacuum casimir-rabi splittings, Phys. Rev. X **8**, 011031 (2018).
- [58] P. D. Nation, J. Suh, and M. P. Blencowe, Ultrastrong optomechanics incorporating the dynamical casimir effect, Phys. Rev. A **93**, 022510 (2016).
- [59] N. F. Del Grosso, F. C. Lombardo, and P. I. Villar, Photon generation via the dynamical casimir effect in an optomechanical cavity as a closed quantum system, Phys. Rev. A **100**, 062516 (2019).
- [60] J. M. Raimond, M. Brune, and S. Haroche, Manipulating quantum entanglement with atoms and photons in a cavity, Rev. Mod. Phys. **73**, 565 (2001).
- [61] A. Reiserer and G. Rempe, Cavity-based quantum networks with single atoms and optical photons, Rev. Mod. Phys. **87**, 1379 (2015).
- [62] M. Mücke, E. Figueroa, J. Bochmann, C. Hahn, K. Murr, S. Ritter, C. J. Villas-Boas, and G. Rempe, Electromagnetically induced transparency with single atoms in a cavity, Nature **465**, 755 (2010).
- [63] X.-H. Bao, A. Reingruber, P. Dietrich, J. Rui, A. Dück, T. Strassel, L. Li, N.-L. Liu, B. Zhao, and J.-W. Pan, Efficient and long-lived quantum memory with cold atoms inside a ring cavity, Nature Physics **8**, 517 (2012).
- [64] R. Reimann, W. Alt, T. Kampschulte, T. Macha, L. Ratschbacher, N. Thau, S. Yoon, and D. Meschede, Cavity-modified collective rayleigh scattering of two atoms, Phys. Rev. Lett. **114**, 023601 (2015).
- [65] X. Zhang, N. Zhu, C.-L. Zou, and H. X. Tang, Optomagnonic whispering gallery microresonators, Phys. Rev. Lett. **117**, 123605 (2016).
- [66] A. Osada, R. Hisatomi, A. Noguchi, Y. Tabuchi, R. Yamazaki, K. Usami, M. Sadgrove, R. Yalla, M. Nomura, and Y. Nakamura, Cavity optomagnonics with spin-orbit coupled photons, Phys. Rev. Lett. **116**, 223601 (2016).
- [67] Y.-P. Gao, X.-F. Liu, T.-J. Wang, C. Cao, and C. Wang, Photon excitation and photon-blockade effects in optomagnonic microcavities, Phys. Rev. A **100**, 043831 (2019).
- [68] E. Almpanis, G. P. Zouros, P. A. Pantazopoulos, K. L. Tsakmakidis, N. Papanikolaou, and N. Stefanou, Spherical optomagnonic microresonators: Triple-resonant photon transitions between zeeman-split mie modes, Phys. Rev. B **101**, 054412 (2020).
- [69] Y.-P. Wang, G.-Q. Zhang, D. Zhang, T.-F. Li, C.-M. Hu, and J. Q. You, Bistability of cavity magnon polaritons, Phys. Rev. Lett. **120**, 057202 (2018).
- [70] M. Li, W. H. P. Pernice, and H. X. Tang, Reactive cavity optical force on microdisk-coupled nanomechanical beam waveguides, Phys. Rev. Lett. **103**, 223901 (2009).
- [71] T. Weiss, C. Bruder, and A. Nunnenkamp, Strong-coupling effects in dissipatively coupled optomechanical systems, New journal of physics **15**, 045017 (2013).
- [72] A. C. Hryciw, M. Wu, B. Khanaliloo, and P. E. Barclay, Tuning of nanocavity optomechanical coupling using a near-field fiber probe, Optica **2**, 491 (2015).
- [73] M. Abdi, P. Degenfeld-Schonburg, M. Sameti, C. Navarrete-Benlloch, and M. J. Hartmann, Dissipative optomechanical preparation of macroscopic quantum superposition states, Phys. Rev. Lett. **116**, 233604 (2016).
- [74] A. Kronwald, F. Marquardt, and A. A. Clerk, Dissipative optomechanical squeezing of light, New Journal of Physics **16**, 063058 (2014).
- [75] S. Huang and G. S. Agarwal, Robust force sensing for a free particle in a dissipative optomechanical system with a parametric amplifier, Phys. Rev. A **95**, 023844 (2017).

- [76] A. Xuereb, R. Schnabel, and K. Hammerer, Dissipative optomechanics in a michelson-sagnac interferometer, *Phys. Rev. Lett.* **107**, 213604 (2011).
- [77] O. Kyriienko, T. C. H. Liew, and I. A. Shelykh, Optomechanics with cavity polaritons: Dissipative coupling and unconventional bistability, *Phys. Rev. Lett.* **112**, 076402 (2014).
- [78] F. Elste, S. M. Girvin, and A. A. Clerk, Quantum noise interference and backaction cooling in cavity nanomechanics, *Phys. Rev. Lett.* **102**, 207209 (2009).
- [79] A. K. Tagantsev, I. V. Sokolov, and E. S. Polzik, Dissipative versus dispersive coupling in quantum optomechanics: Squeezing ability and stability, *Phys. Rev. A* **97**, 063820 (2018).
- [80] C. Regal, J. Teufel, and K. Lehnert, Measuring nanomechanical motion with a microwave cavity interferometer, *Nature Physics* **4**, 555 (2008).
- [81] J. D. Teufel, J. W. Harlow, C. A. Regal, and K. W. Lehnert, Dynamical backaction of microwave fields on a nanomechanical oscillator, *Phys. Rev. Lett.* **101**, 197203 (2008).
- [82] M. Asano, R. Ohta, T. Yamamoto, H. Okamoto, and H. Yamaguchi, An opto-electro-mechanical system based on evanescently-coupled optical microbottle and electromechanical resonator, *Applied Physics Letters* **112**, 201103 (2018).
- [83] M. Wu, A. C. Hryciw, C. Healey, D. P. Lake, H. Jayakumar, M. R. Freeman, J. P. Davis, and P. E. Barclay, Dissipative and dispersive optomechanics in a nanocavity torque sensor, *Phys. Rev. X* **4**, 021052 (2014).
- [84] K. J. Vahala, Optical microcavities, *nature* **424**, 839 (2003).
- [85] M. Pöllinger, D. O'Shea, F. Warken, and A. Rauschenbeutel, Ultrahigh- $q$  tunable whispering-gallery-mode microresonator, *Phys. Rev. Lett.* **103**, 053901 (2009).
- [86] L. Collot, V. Lefevre-Seguín, M. Brune, J. Raimond, and S. Haroche, Very high- $q$  whispering-gallery mode resonances observed on fused silica microspheres, *EPL (Europhysics Letters)* **23**, 327 (1993).
- [87] G. Lin, S. Diallo, R. Henriët, M. Jacquot, and Y. K. Chembo, Barium fluoride whispering-gallery-mode disk-resonator with one billion quality-factor, *Optics Letters* **39**, 6009 (2014).
- [88] H.-Y. Ryu, M. Notomi, G.-H. Kim, and Y.-H. Lee, High quality-factor whispering-gallery mode in the photonic crystal hexagonal disk cavity, *Optics express* **12**, 1708 (2004).
- [89] N. Acharyya and G. Kozyreff, Large  $q$  factor with very small whispering-gallery-mode resonators, *Phys. Rev. Applied* **12**, 014060 (2019).
- [90] W. Xiong, D.-Y. Jin, Y. Qiu, C.-H. Lam, and J. Q. You, Cross-kerr effect on an optomechanical system, *Phys. Rev. A* **93**, 023844 (2016).
- [91] R. Khan, F. Massel, and T. T. Heikkilä, Cross-kerr nonlinearity in optomechanical systems, *Phys. Rev. A* **91**, 043822 (2015).
- [92] J.-S. Zhang, W. Zeng, and A.-X. Chen, Effects of cross-kerr coupling and parametric nonlinearity on normal mode splitting, cooling, and entanglement in optomechanical systems, *Quantum Information Processing* **16**, 163 (2017).
- [93] S.-S. Chen, H. Zhang, Q. Ai, and G.-J. Yang, Phononic entanglement concentration via optomechanical interactions, *Phys. Rev. A* **100**, 052306 (2019).
- [94] F. Zou, L.-B. Fan, J.-F. Huang, and J.-Q. Liao, Enhancement of few-photon optomechanical effects with cross-kerr nonlinearity, *Phys. Rev. A* **99**, 043837 (2019).
- [95] T. T. Heikkilä, F. Massel, J. Tuorila, R. Khan, and M. A. Sillanpää, Enhancing optomechanical coupling via the josephson effect, *Phys. Rev. Lett.* **112**, 203603 (2014).
- [96] N. Makri and D. E. Makarov, Tensor propagator for iterative quantum time evolution of reduced density matrices. i. theory, *The Journal of chemical physics* **102**, 4600 (1995).
- [97] A. Vagov, M. D. Croitoru, M. Glässl, V. M. Axt, and T. Kuhn, Real-time path integrals for quantum dots: Quantum dissipative dynamics with superohmic environment coupling, *Phys. Rev. B* **83**, 094303 (2011).
- [98] I. S. Gradshteyn and I. M. Ryzhik, *Table of integrals, series, and products* (Academic press, 2014).